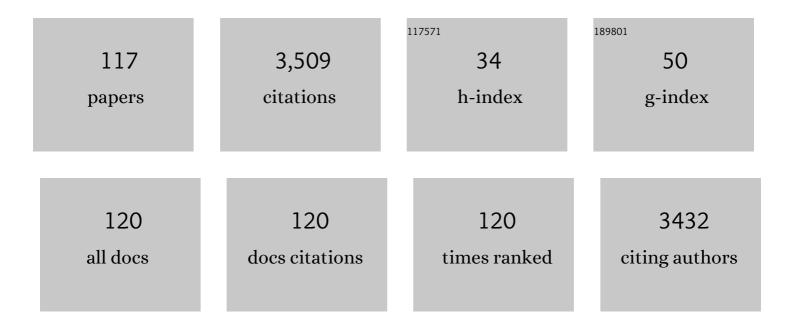
List of Publications by Year in descending order

Source: https://exaly.com/author-pdf/2753599/publications.pdf Version: 2024-02-01



#	Article	IF	CITATIONS
1	Enhanced visible-light photocatalytic activity of strontium-doped zinc oxide nanoparticles. Materials Science in Semiconductor Processing, 2015, 32, 152-159.	1.9	147
2	Optical and electrical properties of p-type Ag-doped ZnO nanostructures. Ceramics International, 2014, 40, 7957-7963.	2.3	140
3	Highly efficient photo-degradation of methyl blue and band gap shift of SnS nanoparticles under different sonication frequencies. Materials Science in Semiconductor Processing, 2015, 32, 172-178.	1.9	92
4	Enhanced ethanol gas-sensing performance of Pb-doped In2O3 nanostructures prepared by sonochemical method. Sensors and Actuators B: Chemical, 2017, 242, 778-791.	4.0	91
5	XPS studies and photocurrent applications of alkali-metals-doped ZnO nanoparticles under visible illumination conditions. Physica E: Low-Dimensional Systems and Nanostructures, 2016, 79, 113-118.	1.3	90
6	Experimental and Theoretical Study of Enhanced Photocatalytic Activity of Mgâ€Doped ZnO NPs and ZnO/rGO Nanocomposites. Chemistry - an Asian Journal, 2018, 13, 194-203.	1.7	83
7	The effect of group-I elements on the structural and optical properties of ZnO nanoparticles. Ceramics International, 2013, 39, 1371-1377.	2.3	80
8	Growth, X-ray peak broadening studies, and optical properties of Mg-doped ZnO nanoparticles. Materials Science in Semiconductor Processing, 2013, 16, 771-777.	1.9	71
9	Enhanced photocatalytic performance of ZnSe/PANI nanocomposites for degradation of organic and inorganic pollutants. Applied Surface Science, 2018, 462, 730-738.	3.1	70
10	SnS nanosheet films deposited via thermal evaporation: The effects of buffer layers on photovoltaic performance. Solar Energy Materials and Solar Cells, 2016, 154, 49-56.	3.0	67
11	Observation of Photoconductivity in Sn-Doped ZnO Nanowires and Their Photoenhanced Field Emission Behavior. Journal of Physical Chemistry C, 2010, 114, 3843-3849.	1.5	63
12	Excellent photocatalytic performance of Zn(1â^'x)MgxO/rGO nanocomposites under natural sunlight irradiation and their photovoltaic and UV detector applications. Materials and Design, 2016, 107, 47-55.	3.3	62
13	CuO and Ag/CuO nanoparticles: Biosynthesis and antibacterial properties. Materials Letters, 2017, 196, 78-82.	1.3	62
14	Photocurrent application of Zn-doped CdS nanostructures grown by thermal evaporation method. Ceramics International, 2016, 42, 1891-1896.	2.3	54
15	Effect of indium concentration on morphology and optical properties of In-doped ZnO nanostructures. Ceramics International, 2012, 38, 6295-6301.	2.3	53
16	Characterization and field emission properties of ZnMgO nanowires fabricated by thermal evaporation process. Solid State Sciences, 2010, 12, 1088-1093.	1.5	50
17	A Comparative Study of the Properties of ZnO Nano/Microstructures Grown using Two Types of Thermal Evaporation Set $\hat{a} \in$ Up Conditions. Chemical Vapor Deposition, 2012, 18, 215-220.	1.4	48
18	The effect of tin sulfide quantum dots size on photocatalytic and photovoltaic performance. Materials Chemistry and Physics, 2017, 195, 187-194.	2.0	47

#	Article	IF	CITATIONS
19	Ultrasonic synthesis of In-doped SnS nanoparticles and their physical properties. Solid State Sciences, 2018, 79, 30-37.	1.5	47
20	Growth, Optical, and Field Emission Properties of Aligned CdS Nanowires. Crystal Growth and Design, 2009, 9, 4157-4162.	1.4	46
21	Optical and electrical properties of p-type Li-doped ZnO nanowires. Superlattices and Microstructures, 2013, 61, 91-96.	1.4	46
22	Electrochemical synthesis of Cu/ZnO nanocomposite films and their efficient field emission behaviour. Applied Surface Science, 2010, 256, 2110-2114.	3.1	45
23	In-doped CuS nanostructures: Ultrasonic synthesis, physical properties, and enhanced photocatalytic behavior. Physica B: Condensed Matter, 2019, 570, 148-156.	1.3	45
24	A sensitive electrochemical nitrate sensor based on polypyrrole coated palladium nanoclusters. Journal of Electroanalytical Chemistry, 2015, 751, 30-36.	1.9	44
25	Effect of Al doping on the structural and optical properties of electrodeposited SnS thin films. Physica Status Solidi (A) Applications and Materials Science, 2016, 213, 1302-1308.	0.8	44
26	Electrochemically synthesis and optoelectronic properties of Pb- and Zn-doped nanostructured SnSe films. Applied Surface Science, 2018, 443, 345-353.	3.1	42
27	Type-II p(SnSe)-n(g-C3N4) heterostructure as a fast visible-light photocatalytic material: Boosted by an efficient interfacial charge transfer of p-n heterojunction. Journal of Alloys and Compounds, 2020, 829, 154436.	2.8	42
28	Influence of lead concentration on morphology and optical properties of Pb-doped ZnO nanowires. Ceramics International, 2013, 39, 9115-9119.	2.3	41
29	Synthesis and characterization of type-II p(CuxSey)/n(g-C3N4) heterojunction with enhanced visible-light photocatalytic performance for degradation of dye pollutants. Colloids and Surfaces A: Physicochemical and Engineering Aspects, 2020, 595, 124656.	2.3	39
30	Nanostructured SnS1â^'xTex thin films: Effect of Te concentration and physical properties. Journal of Alloys and Compounds, 2016, 681, 595-605.	2.8	38
31	Effect of chlorine ion concentration on morphology and optical properties of Cl-doped ZnO nanostructures. Ceramics International, 2012, 38, 5821-5825.	2.3	37
32	Synthesis and characterization of single crystal PbO nanoparticles in a gelatin medium. Ceramics International, 2014, 40, 11699-11703.	2.3	36
33	Electrochemical synthesis of Sn doped ZnO nanowires on zinc foil and their field emission studies. Thin Solid Films, 2010, 519, 184-189.	0.8	35
34	High current density, low threshold field emission from functionalized carbon nanotube bucky paper. Applied Physics Letters, 2010, 97, .	1.5	35
35	Facile synthesis of different morphologies of Te-doped ZnO nanostructures. Ceramics International, 2014, 40, 7737-7743.	2.3	35
36	Annealing temperature of nanostructured SnS on the role of the absorber layer. Materials Science in Semiconductor Processing, 2019, 90, 120-128.	1.9	35

#	Article	IF	CITATIONS
37	Synthesis and characterization of Fe3O4 rose like and spherical/reduced graphene oxide nanosheet composites for lead (II) sensor. Electrochimica Acta, 2015, 169, 126-133.	2.6	32
38	Enhanced photovoltaic performance of tin sulfide nanoparticles by indium doping. MRS Communications, 2016, 6, 421-428.	0.8	32
39	Excellent photocatalytic performance under visible-light irradiation of ZnS/rGO nanocomposites synthesized by a green method. Frontiers of Materials Science, 2016, 10, 385-393.	1.1	31
40	Effect of annealing temperature and graphene concentrations on photovoltaic and NIR-detector applications of PbS/rGO nanocomposites. Ceramics International, 2016, 42, 15209-15216.	2.3	31
41	Broad Spectral Response of Seâ€Doped SnS Nanorods Synthesized through Electrodeposition. ChemElectroChem, 2017, 4, 1478-1486.	1.7	31
42	Surface characterization of Au–ZnO nanowire films. Ceramics International, 2012, 38, 6665-6670.	2.3	30
43	Photocurrent applications of Zn (1â^'x) Cd x O/rGO nanocomposites. Ceramics International, 2016, 42, 7455-7461.	2.3	30
44	Optical, electrical, and photovoltaic properties of PbS thin films by anionic and cationic dopants. Applied Physics A: Materials Science and Processing, 2017, 123, 1.	1.1	30
45	Pb-doped Cu3Se2 nanosheets: Electrochemical synthesis, structural features and optoelectronic properties. Solar Energy, 2018, 171, 508-518.	2.9	30
46	Low temperature growth of aligned ZnO nanowires and their application as field emission cathodes. Materials Chemistry and Physics, 2010, 120, 691-696.	2.0	29
47	An efficient wide range photodetector fabricated using a bilayer Bi ₂ S ₃ /SnS heterojunction thin film. Semiconductor Science and Technology, 2019, 34, 045008.	1.0	29
48	Influence of growth conditions on the electrochemical synthesis of SnS thin films and their optical properties. International Journal of Minerals, Metallurgy and Materials, 2016, 23, 348-357.	2.4	28
49	Electrochemical deposition of nanostructured SnS1â^'xTex thin films and their surface characterization. Journal of Alloys and Compounds, 2017, 694, 1338-1347.	2.8	28
50	Physical properties of Pb-doped CuS nanostructures for optoelectronic applications. Materials Science in Semiconductor Processing, 2021, 123, 105501.	1.9	28
51	Optical properties of group-I-doped ZnO nanowires. Ceramics International, 2014, 40, 4327-4332.	2.3	27
52	Synthesis of Cu–ZnO and C–ZnO nanoneedle arrays on zinc foil by low temperature oxidation route: Effect of buffer layers on growth, optical and field emission properties. Applied Surface Science, 2011, 257, 8366-8372.	3.1	26
53	Electrochemical synthesis and physical properties of Sn-doped CdO nanostructures. Superlattices and Microstructures, 2016, 100, 988-996.	1.4	26
54	Sonochemical synthesis of Cu-doped CdO nanostructures and investigation of their physical properties. Materials Science in Semiconductor Processing, 2018, 74, 210-217.	1.9	26

#	Article	IF	CITATIONS
55	Ultrasound-assisted electrodeposition of Cu3Se2 nanosheets and efficient solar cell performance. Journal of Alloys and Compounds, 2019, 780, 626-633.	2.8	26
56	Field emission studies on electrochemically synthesized ZnO nanowires. Ultramicroscopy, 2009, 109, 418-422.	0.8	25
57	Growth and optical properties of ZnO–In2O3 heterostructure nanowires. Ceramics International, 2013, 39, 5191-5196.	2.3	25
58	Examining the effect of Zn dopant on physical properties of nanostructured SnS thin film by using electrodeposition. Journal of Applied Electrochemistry, 2016, 46, 323-330.	1.5	25
59	Synthesis and characterization of Pb-doped ZnO nanoparticles and their photocatalytic applications. Materials Research Innovations, 2016, 20, 121-127.	1.0	24
60	Charge transportation mechanisms in TiO2/SnS/Ag solar cells. Materials Research Bulletin, 2020, 124, 110727.	2.7	24
61	Influence of process variables on growth of ZnO nanowires by cathodic electrodeposition on zinc substrate. Thin Solid Films, 2009, 517, 6605-6611.	0.8	23
62	Photocurrent Properties of Undoped and Pb-Doped SnS Nanostructures Grown Using Electrodeposition Method. Journal of Electronic Materials, 2015, 44, 4734-4739.	1.0	23
63	Microwave-assisted solvothermal synthesis and optoelectronic properties of γ-MnS nanoparticles. Journal of Materials Science: Materials in Electronics, 2018, 29, 10976-10985.	1.1	21
64	Synthesis and physical properties of un- and Zn-doped Ag2S nanoparticles. Advanced Powder Technology, 2019, 30, 347-358.	2.0	21
65	Optoelectronic Properties of Mixed Sn/Pb Perovskite Solar Cells: The Study of Compressive Strain by Raman Modes. Journal of Physical Chemistry C, 2020, 124, 27136-27147.	1.5	21
66	Synthesis and characterization of PbS mesostructures as an IR detector grown by hydrogen-assisted thermal evaporation. Materials Science in Semiconductor Processing, 2014, 26, 704-709.	1.9	20
67	Al-doped Ag2S nanostructures: Ultrasonic synthesis and physical properties. Ceramics International, 2019, 45, 6175-6182.	2.3	20
68	Microwave-assisted solvothermal synthesis and physical properties of Zn-doped MnS nanoparticles. Solid State Sciences, 2019, 93, 31-36.	1.5	20
69	Tuning crystal phase and morphology of copper selenide nanostructures and their visible-light photocatalytic applications to degrade organic pollutants. Colloids and Surfaces A: Physicochemical and Engineering Aspects, 2020, 586, 124196.	2.3	20
70	Enhanced solar cell performance of P3HT:PCBM by SnS nanoparticles. Solar Energy, 2020, 199, 872-884.	2.9	20
71	Chemical solution deposition of ZnO nanostructure films: Morphology and substrate angle dependency. Ceramics International, 2012, 38, 3649-3657.	2.3	19
72	Improved Synthesis of Reduced Graphene Oxide-Titanium Dioxide Composite with Highly Exposed{001}Facets and Its Photoelectrochemical Response. International Journal of Photoenergy, 2014, 2014, 1-9.	1.4	19

#	Article	IF	CITATIONS
73	Effect of thickness on the optoelectronic properties of electrodeposited nanostructured SnS films. Optical and Quantum Electronics, 2018, 50, 1.	1.5	18
74	Zn-doped Pb/Sn hybrid perovskite solar cells: Towards high photovoltaic performance. Solar Energy, 2022, 236, 63-74.	2.9	18
75	Electrochemical synthesis and surface characterization of hexagonal Cu–ZnO nano-funnel tube films. Ceramics International, 2013, 39, 3715-3720.	2.3	17
76	Influence of synthesis parameters on the physical properties of Cu3Se2 nanostructures using the sonochemical method. Ceramics International, 2019, 45, 16765-16775.	2.3	17
77	Photovoltaic behavior of SnS solar cells under temperature variations. Optik, 2022, 254, 168635.	1.4	17
78	Effect of hydrogen gas on the growth process of PbS nanorods grown by a CVD method. Current Applied Physics, 2014, 14, 1031-1035.	1.1	16
79	UV-assisted sonochemical synthesis and optoelectrical properties of Bi2S3/rGO nanocomposites. Ceramics International, 2019, 45, 13923-13933.	2.3	16
80	Roles of Sn content in physical features and charge transportation mechanism of Pb-Sn binary perovskite solar cells. Solar Energy, 2020, 209, 590-601.	2.9	16
81	Electrodeposition of In-doped SnSe nanoparticles films: Correlation of physical characteristics with solar cell performance. Solid State Sciences, 2020, 108, 106388.	1.5	16
82	Influences of anionic and cationic dopants on the morphology and optical properties of PbS nanostructures. Chinese Physics B, 2014, 23, 108101.	0.7	15
83	Transient photocurrent response of Bi ₂ S ₃ /rGO nanocomposites synthesized by UV-assisted sonication method. Materials Research Express, 2019, 6, 086332.	0.8	15
84	Electro-sonical deposition of nanostructured Sb2Se3 films for optoelectronic applications. Journal of Alloys and Compounds, 2021, 855, 157308.	2.8	15
85	Visible-range and self-powered bilayer p-Si/n-Bi2S3 heterojunction photodetector: The effect of Au buffer layer on the optoelectronics performance. Journal of Alloys and Compounds, 2022, 905, 164119.	2.8	15
86	Synthesis of polypyrrole coated manganese nanowires and their application in hydrogen peroxide detection. Materials Chemistry and Physics, 2013, 141, 298-303.	2.0	14
87	Large-scale and facile fabrication of PbSe nanostructures by selenization of a Pb sheet. Functional Materials Letters, 2015, 08, 1550063.	0.7	14
88	A simple method to fabricate an NIR detector by PbTe nanowires in a large scale. Materials Research Bulletin, 2016, 77, 131-137.	2.7	14
89	Photocurrent application of Cd-doped ZnTe nanowires grown in a large scale by a CVD method. Vacuum, 2016, 123, 131-135.	1.6	14
90	Synthesis and transient photocurrent behavior of Zn-doped In2O3 nanorods. Sensors and Actuators A: Physical, 2017, 265, 246-252.	2.0	14

#	Article	IF	CITATIONS
91	Large-scale and facial fabrication of PbS nanorods by sulfuration of a Pb sheet. Materials Science in Semiconductor Processing, 2014, 21, 98-103.	1.9	13
92	Ultrasonic synthesis of Zn-doped CdO nanostructures and their optoelectronic properties. Transactions of Nonferrous Metals Society of China, 2018, 28, 2255-2264.	1.7	13
93	Improvement visible-light photocatalytic performance of single-crystalline SnSe1±x NPs toward degradation of organic pollutants. Solid State Sciences, 2019, 98, 106044.	1.5	13
94	Optimization of absorber layer for band gap energy moderation of nanostructured SnS thin films. Journal of Materials Science: Materials in Electronics, 2019, 30, 11123-11135.	1.1	13
95	Influence of chemical routes on optical and field emission properties of Au–ZnO nanowire films. Vacuum, 2014, 101, 233-237.	1.6	12
96	Effect of growth condition on structure and optical properties of hybrid Ag-CuO nanomaterials. Advanced Powder Technology, 2016, 27, 2196-2203.	2.0	12
97	Optoelectronic properties of Zn-doped Cu3Se2 nanosheets for photovoltaic application. Ceramics International, 2020, 46, 21978-21988.	2.3	11
98	Sonochemical synthesis of Fe-doped Cu3Se2 nanoparticles: Correlation of the strain and electrical properties for optoelectronics applications. Advanced Powder Technology, 2021, 32, 3412-3424.	2.0	11
99	Electroplating of Ni/Co–pumice multilayer nanocomposite coatings: Effect of current density on crystal texture transformations and corrosion behavior. International Journal of Minerals, Metallurgy and Materials, 2019, 26, 1299-1310.	2.4	10
100	Nanostructured FeS2 films: Influence of effective parameters on electrochemical deposition and characterization of physical properties. Ceramics International, 2021, 47, 21969-21969.	2.3	9
101	Sn–ZnO nanoneedles grown on Zn wire as a pointed field emitter and switching device. Materials Letters, 2013, 111, 181-184.	1.3	8
102	Photovoltaic and photodetector performance of metal telluride nanowires grown by a simple CVD method. Journal of Materials Science: Materials in Electronics, 2017, 28, 4475-4480.	1.1	8
103	Mn-doped Cu3Se2 nanosheets: Impact of physical characteristics on the photovoltaic performance. Materials Research Bulletin, 2020, 132, 111001.	2.7	8
104	Correlation of Physical Features and the Photovoltaic Performance of P3HT:PCBM Solar Cells by Cu-Doped SnS Nanoparticles. Journal of Physical Chemistry C, 2021, 125, 15841-15852.	1.5	8
105	Symmetric strain- and temperature-dependent optoelectronics performance of TiO2/SnS/Ag solar cells. Surfaces and Interfaces, 2021, 25, 101223.	1.5	7
106	Electrodeposition of nanostructured FeS2 films: The effect of Sn concentrations on the optoelectronic performance. Solid State Sciences, 2021, 120, 106722.	1.5	6
107	Electrodeposition of Cu–ZnO nanocomposites: Effect of growth conditions on morphologies and surface properties. Materials Science in Semiconductor Processing, 2014, 27, 507-514.	1.9	5
108	Synthesis of Te-doped ZnO nanowires with promising field emission behavior. RSC Advances, 2016, 6, 115335-115344.	1.7	5

#	Article	IF	CITATIONS
109	Investigation of the optoelectronic behavior of Pb-doped CdO nanostructures. Applied Nanoscience (Switzerland), 2018, 8, 937-948.	1.6	5
110	Field Emission Properties of Al-Doped ZnO Nanostructures. Journal of Nano Research, 2009, 5, 231-237.	0.8	4
111	The Role of Ag/Al Electrodes in the Improvement of PEDOT:PSS/P3HT:PCBM Solar Cells Performance. IEEE Journal of Photovoltaics, 2020, 10, 1346-1352.	1.5	4
112	Optoelectronic properties of nanostructured Sb2Se3 films synthesized by electrodeposition method: Effect of Zn concentrations. Sensors and Actuators A: Physical, 2022, 344, 113750.	2.0	4
113	Effect of annealing process on the growth and surface properties of Au–ZnO nanowire films grown by chemical routes. Ceramics International, 2013, 39, 7577-7581.	2.3	3
114	Nanoarchitectonics of SnSe with the impacts of ultrasonic powers and ultraviolet radiations on physical and optoelectronic properties. Advanced Powder Technology, 2022, 33, 103517.	2.0	3
115	Effect of ultrasonic irradiation time on the physical and optoelectronic properties of SnSe nanorods. Surfaces and Interfaces, 2021, 27, 101433.	1.5	2
116	The Ecotoxicity of Nanoparticles Co2O3 and Fe2O3 on Daphnia magna in Freshwater. Journal of Water Chemistry and Technology, 2021, 43, 509-516.	0.2	2
117	The effect of pumice reinforcing particles on the corrosion-and wear-resistance of Ni/Co-pumice bilayer coatings by electroplating. Materials Research Express, 2019, 6, 126506.	0.8	1